The marine lipopeptide somocystinamide A triggers apoptosis via caspase 8

Wolf Wrasidlo*[†], Ainhoa Mielgo*[‡], Vicente A. Torres*[‡], Simone Barbero*[‡], Konstantin Stoletov*[‡], Takashi L. Suyama[§], Richard L. Klemke*[‡], William H. Gerwick*[§¶], Dennis A. Carson*[†], and Dwayne G. Stupack*[†‡]

[‡]Department of Pathology, University of California at San Diego (UCSD) School of Medicine, and *Moores UCSD Cancer Center, 3855 Health Sciences Drive, La Jolla, CA 92093-0803; [¶]Skaggs School of Pharmacy and Pharmaceutical Sciences, University of California at San Diego, 9500 Gilman Drive, La Jolla, CA 92093; and [§]Scripps Institute of Oceanography, 8602 La Jolla Shores Drive, La Jolla, CA 92037

Screening for novel anticancer drugs in chemical libraries isolated from marine organisms, we identified the lipopeptide somocystinamide A (ScA) as a pluripotent inhibitor of angiogenesis and tumor cell proliferation. The antiproliferative activity was largely attributable to induction of programmed cell death. Sensitivity to ScA was significantly increased among cells expressing caspase 8, whereas siRNA knockdown of caspase 8 increased survival after exposure to ScA. ScA rapidly and efficiently partitioned into liposomes while retaining full antiproliferative activity. Consistent with the induction of apoptosis via the lipid compartment, we noted accumulation and aggregation of ceramide in treated cells and subsequent colocalization with caspase 8. Angiogenic endothelial cells were extremely sensitive to ScA. Picomolar concentrations of ScA disrupted proliferation and endothelial tubule formation *in vitro*. Systemic treatment of zebrafish or local treatment of the chick chorioallantoic membrane with ScA resulted in dose-dependent inhibition of angiogenesis, whereas topical treatment blocked tumor growth among caspase-8-expressing tumors. Together, the results reveal an unexpected mechanism of action for this unique lipopeptide and suggest future development of this and similar agents as antiangiogenesis and anticancer drugs.

angiogenesis | cancer | nanoparticle

Massive efforts to develop improved anticancer drugs have focused on high-throughput screening of large compound libraries. This is, in part, because of the relative lack of success achieved to date by using structure-based drug design against tumor targets. However, it is noteworthy that many anticancer drugs presently used in clinical practice are natural products (such as taxoids, vinca alkaloids, or anthracyclines) or are derivatives of natural products (such as etoposides) (1). Therefore, the continued analysis of natural sources remains likely to reveal new and unexpected compounds with potential medical applications, which is supported not only by these prior successes but also by recent assessments of biodiversity (2–4).

In this respect, metabolites from marine microorganisms provide a significant resource for the discovery of novel, small molecules for pharmaceutical and biomedical applications (5, 6). *Lyngbya majuscula* in particular has been extensively studied and has produced >250 different compounds with diverse structural features (7, 8). This diversity is in part attributable to the fact that a major theme in *L. majuscula* biochemistry relies on the production of metabolites via polyketide synthases and nonribosomal peptide synthetases within specialized biosynthetic pathways (9). Here, we describe the activity and mechanism of action of a lipopeptide derived from *L. majuscula*, somocystinamide A (ScA), that potently induces apoptosis in tumor and angiogenic endothelial cells. Although ScA initiates apoptosis via both the intrinsic and extrinsic pathways, the more sensitive pathway involves activation of caspase 8, which requires concentrations in the low nanomolar range and below, to initiate alterations in the cell membrane and apoptosis. The selective activation of the caspase 8 pathway by a small molecule is promising, because few currently used anticancer agents have this

property. Many malignant tumors maintain expression of caspase 8, suggesting it may be an attractive target for tumor suppression (10). Importantly, ScA possesses intrinsically attractive chemical properties, including a unique but readily synthesized structure and the capacity to spontaneously incorporate into lipid nanoplatforms while retaining proapoptotic activity. It would seem that such properties may be an asset for delivery via targeted nanoparticles, which is currently under development for clinical use.

Results

ScA Induces Apoptosis Selectively via Caspase 8. In initial studies, we reported that ScA isolated from mixed assemblage *L. majuscula/Schizothrix* species yielded modest cytotoxic effects against a murine neuroblastoma cell line (11). Initial studies were somewhat limited by the relatively low abundance of this compound. In continuing investigations, we now document that freshly isolated ScA shows potent antiproliferative activity against a number of human tumor cells (Table 1). Microscopic examination reveals that the loss of proliferation is associated with a "blebbing" morphology (Fig. 1 *A* and *B*), whereas biochemical analysis revealed proteolytic processing of cellular proteins, such as caspase 8 and poly(ADP-ribose) polymerase (PARP), that are hallmark indicators of apoptosis (Fig. 1*C*). To determine whether caspase 8 expression could account for increased ScA activity, we examined the ability of ScA to induce apoptosis in wild-type Jurkat cells or those deficient in caspase 8. Compared with wild-type cells, apoptosis was dramatically decreased among caspase-8-deficient Jurkat cells exposed to ScA (Fig. 1*D*). Extending these studies, we knocked down expression of caspase 8 (≈80%) by using a short-hairpin RNA (shRNA) approach in the A549 cell line and found a 5-fold loss in sensitivity to ScA (Fig. 1*E*). Finally, we also tested NB7 neuroblastoma tumor cells, which are deficient for caspase 8 expression, and the matched sister line, NB7C8, which is reconstituted for physiological levels of caspase 8 expression (12). In this case, the expression of caspase 8 increased the potency (IC_{50}) of ScA by 50-fold (Fig. 1*F*). The results implicate caspase 8 as an effector of apoptosis after ScA treatment.

Caspase 8 is an effector of death receptor (DR)-mediated apoptosis after DR ligation by an appropriate agonist, which triggers the recruitment of the adaptor protein FADD and subsequent formation of the death-inducing signaling complex

APPLIED BIOLOGICAL SCIENCES

Table 1. Activity of ScA versus tumor cell lines

Cell line	Type	IC$_{50}$
Jurkat	Leukemia	3 nM
CEM	Leukemia	14 nM
A549	Lung carcinoma	46 nM
Molt4	T cell leukemia	60 nM
MCF-7	Breast carcinoma	210 nM
NB7	Neuroblastoma	810 nM
PC3	Prostate carcinoma	970 nM
M21	Melanoma	1.3 μM
U266	Myeloma	5.8 μM

(13). Accordingly, Jurkat cells lacking FADD were protected from ScA-mediated killing (Fig. 1D), implicating DR-mediated killing in this process. However, NB7C8 cells are resistant to DR-mediated killing (12), and similarly A549 cells do not undergo Fas-mediated apoptosis (ref. 14; our unpublished results), although both cell lines were sensitive to ScA-induced killing. In agreement with these results, the addition of the Fas agonist CH11 did not cooperate with ScA to promote cell death [see supporting information (SI)]. However, DR "ligation" is not strictly required for apoptosis induced by DRs; rather, it appears that ligand-mediated redistribution of membrane components may be critical to trigger cell death (15–17).

ScA Partitions into Phospholipids and Alters Membrane Structure.
The delivery of drugs via liposomes is clinically relevant (18). Because ScA is a lipophilic compound (logP = 10.3), we assessed the capacity of ScA to partition from liquid phase into 100-nm liposomes (nanosomes). Remarkably, interchelation of ScA within the nanosomes was essentially complete within 30 min, with no residual unincorporated drug detected (data not shown). Testing whether the liposome-borne ScA maintained cytotoxic activity, we found that apoptosis induced by treatment of cells with ScA nanosomes mimicked treatments with ScA as a "free" compound (Fig. 2B). Treatment with control, unloaded nanosomes had no effect on cell viability. Together, these results support the potential for future nanosome-based delivery of ScA *in vivo*, whereas implicating the lipid compartment in ScA-mediated cell death.

In this respect, it is known that alterations to the cell lipid compartment can promote caspase-mediated cell killing. For example, ceramide-enriched membrane domains can promote DR clustering and activation of caspase 8 (17, 19, 20), whereas treatment with arachidonic acid can mediate caspase-3-dependent cell death (21). Therefore, we examined the A549 cells for evidence of alteration to the lipid compartment after exposure to ScA. Interestingly, we observed an accumulation, and aggregation, of cell surface ceramide (Fig. 2B, red channel) that was absent among cells treated with diluent (our unpublished results) or those treated with arachidonic acid (control) (Fig. 2B). This result supported the notion that ScA acted via alterations to the plasma membrane. To evaluate whether observed alterations to membrane lipid distribution corresponded to interactions with apoptotic effectors, in particular caspase 8, we next examined whether these aggregated "clusters" of ceramide in the membrane colocalized with this caspase (Fig. 2B, green channel; colocalization is shown in the yellow channel). The results supported the notion that ScA partitions within cell membranes, alters the lipid compartment and induces the external death pathway in susceptible cells. Although ceramide was used as a reporter of changes within the organization of the lipid compartment, it remains unclear which lipids (if any) directly contribute to apoptosis. However,
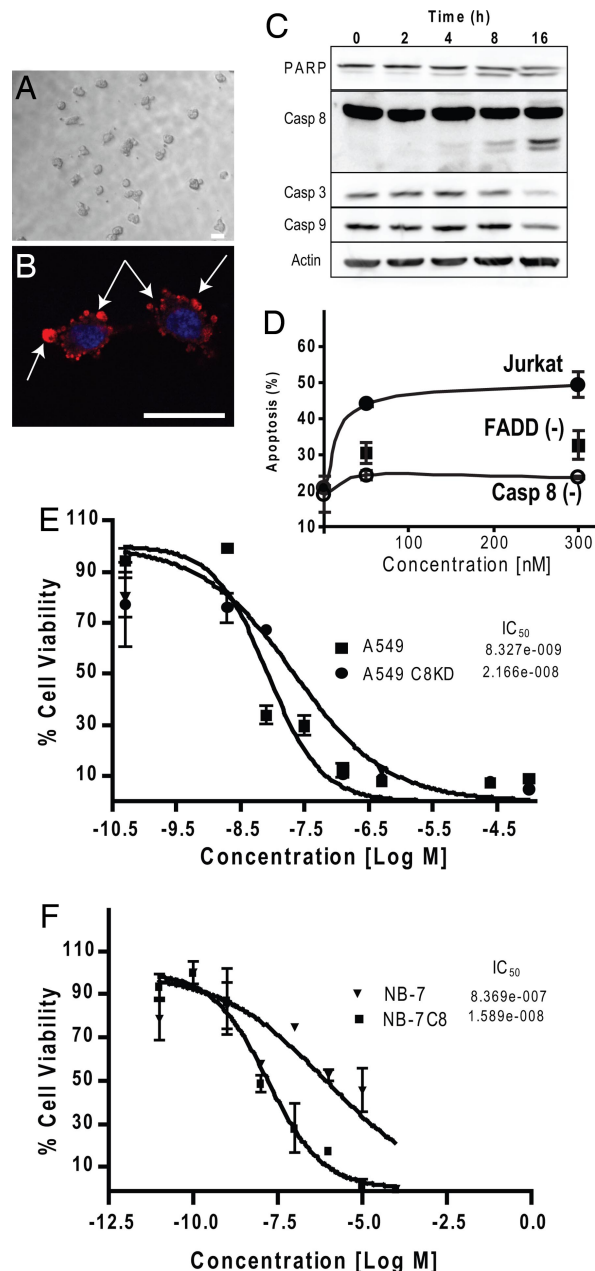
Fig. 1. ScA induces apoptosis selectively via caspase-8-dependent mechanisms. (A) Treatment of A549 cells with 100 nM ScA induces a blebbing morphology, as observed via bright-field microscopy. (B) A549 cells were fixed and costained with antibodies directed against ceramide (red channel). (Scale bars in A and B: 25 μM.) Arrows indicate regions of blebbing. The nuclear compartment was visualized by using DAPI to stain DNA (blue channel). The assessments were performed 2 h after treatment with 300 nM ScA. (C) Immunoblot analysis of Jurkat cells was performed after treatment with 100 nM ScA. Then, 25 μg of cell lysates was probed for caspases 8, 3, and 9, for PARP, and for actin (loading control) as indicated. (D) Caspase 8-deficient (Casp 8−), FADD-deficient (FADD−), or parental Jurkat cells (Jurkat) were incubated with 50 or 300 nM for 6 h and analyzed for the presence of apoptotic cells via FACS analysis of DNA content. Results shown are the mean and standard error of triplicate determinations. (E) A549 cells subjected to lentivirus-delivered shRNA-mediated knockdown of caspase 8 or treated with a scrambled shRNA lentivirus. Cells then were cultured in the presence of increasing doses of ScA, as indicated. Viability was measured by XTT assay after 72 h and normalized to controls not treated with drug. (F) Similarly, the viability of neuroblastoma cultures deficient in caspase expression, or reconstituted for caspase 8 expression, was determined as for the A549 cells above. Both experiments are representative, with each point shown the mean ± SE of triplicate wells.
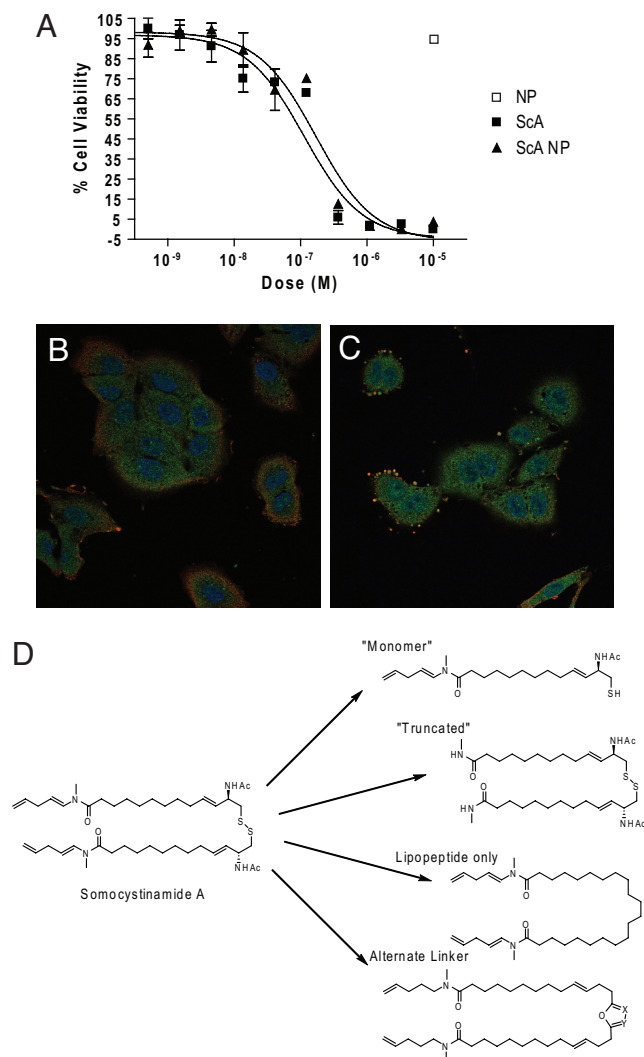
Fig. 2. ScA partitions into the lipid compartment. (*A*) ScA was mixed with DOPE:cholesterol:DSPC:DSPE-mPEG to form liposomes, as described in *Materials and Methods*. ScA completely partitioned into the lipid nanosomes, which had an effective diameter of 109 nm and a polydispersity of 0.205. A549 cells were cultured with free ScA added in DMSO diluent or with ScA incorporated into nanosomes, and cell viability was assessed by XTT assay as described above. (*B* and *C*) A549 cells were stained with anti-ceramide (red channel), DAPI (blue channel), and anti-caspase 8 (green channel) 30 min after treatment with 300 nM arachidonic acid, a control lipid (*B*), or 300 nM ScA (*C*). Colocalization of the green and red channels is shown by the merge (yellow signal). (*D*) A limited structure–function analysis of the required elements for ScA (shown at left) activity was performed. Derivatives of ScA synthesized or derived included a "monomeric" form (with <0.1% activity) and forms in which the disulfide was replaced with alternative linkers, which showed no activity below 50 μM. A "truncated" lipopeptide that maintained the disulfide linkage also lacked activity below 50 μM.

it was not simply the lipophilic nature of ScA that resulted in proapoptotic activity. ScA is a disulfide-linked lipopeptide dimer (Fig. 2*C*), and in parallel structure–function studies we found that individual monomers retained essentially no ability (<0.1% potency) to induce apoptosis. Similarly, chemical modification of either the lipopeptide tail of the molecule or manipulations of the disulfide bond abrogated all tumoricidal activity of the compound. Thus, the combination of lipopeptide and disulfide moieties appears critical to ScA activity.

Antiangiogenic and Antitumoral Effects of ScA. Angiogenic endothelial cells are susceptible to apoptosis initiated by caspase 8

(20, 22, 23). We therefore tested the effect of ScA treatment on endothelial cells *in vitro* and *in vivo*. Cultured endothelial cells were extremely sensitive to ScA (Fig. 3*A*), with an IC_{50} in the picomolar range. In agreement with these results, we found that ScA potently blocked endothelial cell tube formation *in vitro* (Fig. 3*B*), suggesting that ScA might act both on endothelial and on tumor cells *in vivo*.

To test this, we first examined whether systemic exposure to ScA blocked developmental angiogenesis in zebrafish. During development of the zebrafish, intersegmental vessels sprout and grow upwards from the dorsal aorta, and then the tips join to form a dorsal vein (Fig. 4*A*). In a dose-dependent manner (Fig. 4 *B–F*), ScA blocked blood vessel growth and angiogenesis, although all of the fish remained viable during the 24-h period of the study. Similarly, local introduction of ScA into the chick chorioallantoic membrane potently blocked growth-factor-induced angiogenesis (Fig. 4*G*). The results demonstrate the sensitivity of endothelial cells to ScA *in vivo*, in agreement with our observations *in vitro*, and indicate that ScA acts as an antiangiogenic agent. However, it was not clear whether ScA could act directly on tumor cells *in vivo*.

To tested the capacity of ScA to directly inhibit tumor growth *in vivo*, neuroblastoma tumors expressing (or lacking) caspase 8 were seeded into the chick chorioallantoic membrane, and a tumor mass was allowed to establish for 3 days. Tumors then were treated topically with 100 pmol of ScA and allowed to grow a further 5 days before being harvested. In this case, we observed an inhibition of tumor growth selectively in the caspase-8-expressing tumor cells. The results show that, in addition to an antiangiogenic effect, low levels of ScA also can act to inhibit the growth of caspase-8-expressing tumor cells.

Discussion

The genetic diversity in the world's oceans recently has become more widely appreciated (2–4, 24, 25). In particular, the diversity of biochemical matter that arises from unique and previously uncharacterized metabolic pathways holds promise for the development of new compounds in the treatment of human malignancy. This study focuses on the activity of ScA, a lipopeptide derived from the cyanobacteria *L. majuscula* (26, 27). We show here that ScA selectively activates a caspase-8-dependent cell death pathway. Interestingly, apoptosis occurs among tumor lines that are normally resistant to treatment with DR agonists that act via caspase 8, which is of particular interest because many tumors tend to maintain caspase 8 expression, likely because of its ability also to fulfill nonapoptotic roles (10, 28), but are resistant to DR-mediated killing (29). Other natural products, including the complex heterocycle gambogic acid (30) and the related kaurene diterpene (31), also activate caspase-8-dependent killing. Although gambogic acid is structurally unrelated to ScA and acts via distinct molecular pathways (30), the shared property of caspase 8 activation is interesting, and it is conceivable that such compounds could function as defensive adaptations (9).
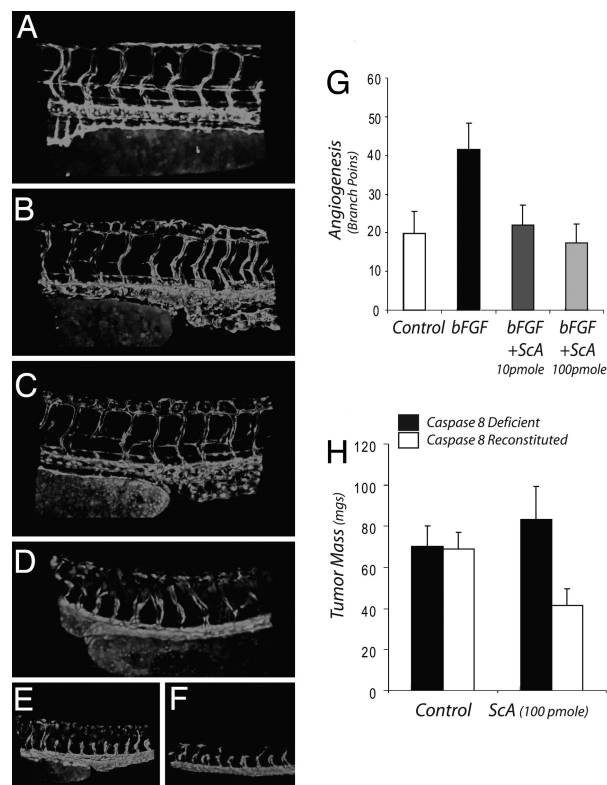
ScA induces alterations in the plasma membrane lipid compartment, as indicated by clustering of ceramide on the cell surface associated with activation of caspase 8 and cell death. At micromolar concentrations, ScA can induce cell death via caspase-8-independent pathways, as shown by its capacity to induce apoptosis in caspase-8-deficient cells. This finding is in agreement with other lipid agents, such as ceramide, which can induce apoptosis via several different actions (19, 32). Nonetheless, the cytotoxic actions of ScA at nanomolar and picomolar concentrations are caspase-8-dependent. Our results group the cell lines examined into two categories: those that are sensitive in the lower nanomolar ranges and those in which near-micromolar and above concentrations are required to induce cell death (Table 1). All of the more sensitive lines can be killed by caspase-8-mediated pathways. However, we expect that metabolic pathways that regulate the lipid composition
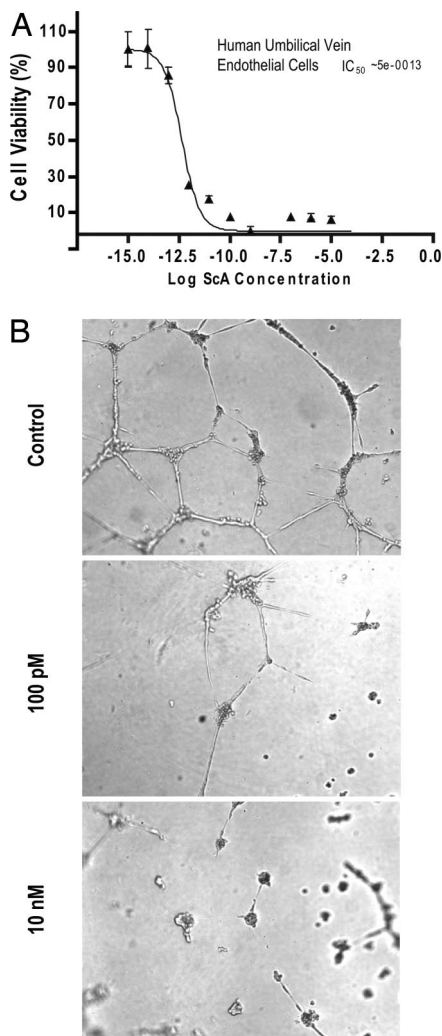
Fig. 3. Endothelial cells are highly sensitive to ScA. (*A*) Human endothelial cells were incubated with ScA at decreasing concentrations, as shown, and viability was assessed by XTT assay after 72 h. Data shown are the mean ± SE of triplicate wells from a representative experiment. (*B*) Human endothelial cells were plated on Matrigel-coated surfaces and allowed to form tubules for 48 h in the presence of DMSO diluent (*Top*). When ScA was added (*Middle* and *Bottom*) cell viability was compromised, and endothelial cell tube formation was disrupted in dose-dependent manner.

Fig. 4. Antiangiogenic and antitumor activity of ScA. (*A*–*F*) Transgenic Tg(fli1:EGFP) zebrafish embryos in which GFP is expressed in endothelial cells were incubated without (*A*) or with increasing concentrations of ScA: 80 nM (*B*), 160 nM (*C*), 300 nM (*D*) 1.6 μM (*E*), or 3 μM (*F*). Blood vessel morphology was recorded by fluorescence microscopy. (*G*) Filter disks impregnated with 100 ng of basic FGF were placed on the chorioallantoic membrane of 11-day-old chicks to induce angiogenesis in the absence or presence of ScA, as shown. After 72 h, disks were removed and the vascularity of the underlying cho-rioallantoic membrane determined by direct counting of branch points using a dissecting microscope. (*H*) NB7 neuroblastoma cells lacking caspase 8 (filled bar) or NB7C8 cells reconstituted for caspase 8 expression (open bars) were seeded into 10-day-old chick chorioallantoic membranes to form tumors. After 72 h, ScA was added topically to each growing tumor mass. Tumors were harvested and resected on day 8, and mass (wet weight) was determined. Data shown is the mean ± SD ($n = 8$–12). The mass of the NB7C8 is significantly decreased ($P < 0.002$).

of the plasma membrane will also act as independent factors that can modulate cell sensitivity to ScA.

ScA contains a disulfide bond that is anticipated to be reduced upon exposure to the inner leaflet of the plasma membrane. However, it is not yet clear whether covalent modification of membrane components by ScA is necessary to activate (or inactivate) ScA-mediated killing. ScA does represent an uncommon structure among compounds isolated from marine cyanobacteria, containing a disulfide moiety and lipopeptide tails, and the cytotoxic activity of ScA requires both lipopeptide and disulfide moieties to initiate caspase-8-dependent death. Truncation of the lipopeptide, or reduction or substitution of the sulfhydryl bonds, abrogated the cytocidal activity of ScA. However, ScA integrated into nanosomes maintained full activity, suggesting an alternative mechanism for delivery in which ScA would be sequestered and protected within a hydrophobic environment, which may be particularly desirable for *in vivo* applications, based on the ability of liposomes to stabilize and provide a targeting function for ScA. For example, interchelation within nanosomes would be expected to

protect the disulfide bond moiety from metabolic degradation after administration *in vivo*. Thus, nanosomes are an attractive candidate for preclinical delivery of ScA.

Synthesis of ScA involves known organic chemistry reactions and can be accomplished via more than one approach. Currently, we are investigating two distinct reaction schemes to optimize yield and purity for future large-scale production. Storage of ScA in an inert dry atmosphere is anticipated to be necessary to avoid eventual hydrolytic degradation of the unsaturated amide, but the compound is otherwise quite stable. Similarly, the production of the nanosomes involves the assembly from commercially available structural and targeting components, and occurs in quantitative yields via standard liposome production techniques. Thus, ScA represents an active natural compound that appears unencumbered by issues with complex synthesis or upscaling commonly associated with natural products.

The optimization of targetable nanoplatforms that home to specific tumor or vascular beds is rapidly proceeding (33). This therapeutic approach will benefit from both pro-drug approaches and from drugs, such as ScA, that show limited solubility in aqueous media and act directly at the plasma

Wrasidlo *et al.*

membrane of susceptible cells. Toxic and relatively insoluble drugs, such as taxols, may find advantages conferred by nano-platform-mediated delivery. Similarly, we expect that the ability of ScA to readily partition within the nanosome lipid component is advantageous for the targeted delivery of this compound to tumors. The targeted nanosome strategy overcomes some issues in terms of solubility and metabolism of ScA while in circulation. In turn, drugs such as ScA do not compete for interior "cargo" space designated for soluble drug payloads. We speculate that such approaches therefore may represent an efficient design for the delivery of combination therapies. Given the sensitivity of proliferating endothelial cells to ScA, it is likely that targeted delivery to cells of the vascular compartment will promote a potent and specific antiangiogenic response.

Materials and Methods

Confocal Microscopy. For confocal analysis, A549 cells were seeded on glass coverslips, treated with ScA, DMSO, or arachidonic acid (controls) at 1 or 0.1 μM concentration for 30 min or 6 h. After treatment, the cells were fixed for 10 min at room temperature with 4% paraformaldehyde, washed twice with PBS, permeabilized for 2 min at room temperature with 0.1% Triton in PBS, and blocked for 30 min with sterile 2% BSA in PBS. The staining was performed at room temperature for 2 h, with mouse monoclonal anti-human ceramide (Alexis) and rabbit anti-human caspase 8 (BD PharMingen) antibodies followed by secondary goat anti-mouse Alexa Fluor 568 and goat anti-rabbit Alexa Fluor 488 antibodies (Invitrogen). The blue DNA binding dye TOPRO-3 (Molecular Probes) was added together with the secondary antibodies. The cells were washed three times with PBS between the different incubation steps, and the incubation with the secondary fluorescently labeled antibodies was performed in the dark. All antibodies were diluted in PBS. Confocal images were recorded on a Nikon Eclipse C1 confocal microscope.

Cell Lines. Cells and cell lines were maintained in either DMEM or RPMI medium 1640 supplemented with 10% FCS. The caspase-deficient NB7 neuroblastoma cells have been described in ref. 34. Caspase-8-deficient and reconstituted Jurkat cells were provided by Steve Hedrick (University of California at San Diego). Silencing of caspase 8 gene expression in the A549 cells was performed through the use of delivering shRNA in a lentiviral format. Briefly, 293 T cells were transfected with caspase 8 (Open Biosystems) or scrambled (Addgene) shRNAs in pLKO.1 lentiviral vector, together with lentiviral packaging plasmids (PMLDL, VSV-G, and RSV-REV) using fugene6. The ratio of target shRNAs and packaging plasmids was shRNA/PMLDL/VSV-G/RSV-REV at 10/10/6/4 μg. Lentiviral supernatants from 293 T cells were harvested after 48 h and used to infect A549 cells. Viral constructs were incubated for 24 h with A549 cell lines before replacing media with selective media containing puromycin (1 μg/ml). The suppression of caspase 8 was verified by Western blotting analysis.

Cytotoxicity Assay. Cytotoxicity of ScA was assessed by using the XTT cell proliferation assay. Briefly, cells were plated on 96-well plates (5,000 per well) and incubated overnight at 37°C to allow for attachment and spreading. After 24 h, ScA was added from a DMSO stock, previously frozen at −80°C, as added directly from serial dilutions in DMSO at concentrations ranging from 100 μM to 100 fM. After 72 h, XTT (Aldrich Chemicals) was added to a final concentration of 250 μg per well. The plates then were incubated under standard tissue culture conditions until the control wells (DMSO) reached an OD value between 1.0 and 1.5. as measured at 450 nm with a microtiter plate reader. The cell viability–drug dilution profiles were obtained from sigma plots, and drug concentrations that inhibited growth by 50% were calculated from multiple runs (IC_{50}).

Preparation of Liposomes. Cholesterol:1,2-dioleoyl-*sn*-glycero-3-phosphoethanolamine (DOPE):1,2-dioleoyl-*sn*-glycero-3-phosphocholine (DSPC):scA:1,2-dioleoyl-*sn*-glycero-3-phosphoethanolamine-*N*-[methoxy(polyethyleneglycol)-

2000] ammonium salt (DSPE-mPEG) (in 1:1:1:0.16:0.16 molar ratio) in chloroform were taken in 30-ml glass culture tubes, dried under a stream of nitrogen gas, and vacuum-desiccated for a minimum of 6 h to remove any residual organic solvent. The dried lipid film was hydrated in sterile deionized water in a total volume of 1 ml for a minimum of 12 h. Liposomes were vortexed for 2–3 min to remove any adhering lipid film and sonicated in a bath sonicator (ULTRAsonik 28X) for 2–3 min at room temperature to produce multilamellar vesicles (MLVs). MLVs then were sonicated with a Ti-probe (using a Branson 450 Sonifier at 100% duty cycle and 25 W output power) in an ice bath for 1–2 min to produce small unilamellar vesicles (SUVs) as indicated by the formation of a clear translucent solution. The solution was pressure-filtered in sequence through 200-nm and then 100-nm nucelopore polycarbonate membranes to obtain liposome nanoparticles of 100 nm with a polydispersity factor of <0.1.

Endothelial Cell Tube Formation. Next, 96-well plates were coated with 200 μl of Matrigel per well and stored at 4°C until use. Human umbilical vein endothelial cells (HUVECs) were harvested, and cell suspensions were prepared at a density of 200,000 per ml, and added at 100 μl per well to the plates. ScA in DMSO were added to each well at 10 nM, 100 pM, and 1 pM concentrations with 1% DMSO as control. The plates were incubated at 37°C under standard incubator conditions, and the results were observed microscopically for tube formation.

Zebrafish Experiments. Blood vessel formation in zebrafish was as follows. Transgenic Tg(fli1:EGFP) zebrafish embryos were purchased from The Zebrafish Model Organism Database (www.zfin.org) as reported in ref. 35. Adult fish and embryos were maintained according to *Zebrafish: A Practical Approach* (36). ScA as a DMSO stock solution was diluted directly into the water, and zebrafish intersegmental vessels were imaged with a Nikon c1-si confocal microscope after the times specified. Raw image datasets were processed by using Imaris 3D image analysis software (www.bitplane.com). All animal procedures were conducted in accordance with all appropriate regulatory standards under protocol S06008 approved by the UCSD Institutional Animal Care and Use Committee.

Chick Chorioallantoic Membrane Studies. The chorioallantoic membrane studies were performed by using 10-day-old chick embryos as described in ref. 37. For the tumor studies, 5×10^6 NB7 or NB7C8 neuroblastoma tumor cells were seeded into the chorioallantoic membranes on 10-day-old embryos and the tumor allowed to develop until day 18 (12).

Western Blotting Analysis. Cells were treated as indicated and extracts were prepared by lysis in RIPA buffer (100 mM Tris, pH 7.5/150 mM NaCl/1 mM EDTA/1% deoxycholate/1% Triton X-100/0.1% SDS/50 mM NaF/complete protease inhibitor; Roche Molecular Biochemicals) on ice. Cell extracts (25 μg) were resolved by 8% SDS/PAGE, transferred to nitrocellulose, and probed with antibodies. Caspase 8 was probed with polyclonal antibody from (Millipore) or affinity-purified catalytic domain-specific antisera (C8–531) prepared at UCSD. Caspase-3 (MAB4703, 1:500; Chemicon), caspase 9 (sc17784, 1:100; Santa Cruz Biotechnology), actin (1:5,000; Sigma), and PARP (sc556493, 1:500; Santa Cruz Biotechnology) were probed with mouse monoclonal antibodies. Bound antibodies were detected with horseradish peroxidase-conjugated secondary antibodies (BioRad) and the ECL system (Pierce).

FACS Analysis. Cell viability was analyzed by flow cytometry after propidium iodide (PI) staining, as described in ref. 38. Briefly, after each treatment, cells were harvested in ice-cold PBS, washed two times in PBS at 4°C, and resuspended in 10 μg/ml PI. The extent of apoptosis was determined by plotting PI fluorescence versus the forward-scatter parameter with Cell Quest software.

1. Newman DJ, Cragg GM (2007) Natural products as sources of new drugs over the last 25 years. *J Nat Prod* 70:461–477.
2. Venter JC, *et al.* (2004) Environmental genome shotgun sequencing of the Sargasso Sea. *Science* 304:66–74.
3. Yooseph S, *et al.* (2007) The Sorcerer II Global Ocean Sampling expedition: Expanding the universe of protein families. *PLoS Biol* 5:e16.
4. Rusch DB, *et al.* (2007) The Sorcerer II Global Ocean Sampling expedition: Northwest Atlantic through eastern tropical Pacific. *PLoS Biol* 5:e77.
5. Fenical W, Sethna K, Lloyd GK (2002) Marine microorganisms as a developing resource for drug discovery. *Pharmaceutical News* 489–494.
6. Kim J, Park EJ (2002) Cytotoxic anticancer candidates from natural resources. *Curr Med Chem Anticancer Agents* 2:485–537.
7. Van Wagoner R, Drummond AK, Wright JLC (2007) Biogenetic diversity of cyanobacterial metabolites. *Adv Appl Microbio* 61:89–217.
8. Gerwick WH, Tan LT, Sitachitta N (2001) Nitrogen-containing metabolites from marine cyanobacteria. *The Alkaloids*, ed Cordell G (Academic, San Diego), Vol 57, pp 75–184.
9. Moore RE (1996) Cyclic peptides and depsipeptides from cyanobacteria: A review. *J Ind Microbiol* 16:134–143.
10. Barnhart BC, *et al.* (2004) CD95 ligand induces motility and invasiveness of apoptosis-resistant tumor cells. *EMBO J* 23:3175–3185.

11. Nogle LM, Gerwick WH (2002) Somocystinamide A, a novel cytotoxic disulfide dimer from a Fijian marine cyanobacterial mixed assemblage. *Org Lett* 4:1095–1098.
12. Stupack DG, *et al*. (2006) Potentiation of neuroblastoma metastasis by loss of caspase-8. *Nature* 439:95–99.
13. Peter ME, Krammer PH (2003) The CD95(APO-1/Fas) DISC and beyond. *Cell Death Differ* 10:26–35.
14. O'Donnell DR, Milligan L, Stark JM (1999) Induction of CD95 (Fas) and apoptosis in respiratory epithelial cell cultures following respiratory syncytial virus infection. *Virology* 257:198–207.
15. Muppidi JR, Siegel RM (2004) Ligand-independent redistribution of Fas (CD95) into lipid rafts mediates clonotypic T cell death. *Nat Immunol* 5:182–189.
16. Malorni W, Giammarioli AM, Garofalo T, Sorice M (2007) Dynamics of lipid raft components during lymphocyte apoptosis: The paradigmatic role of GD3. *Apoptosis* 12:941–949.
17. Elyassaki W, Wu S (2006) Lipid rafts mediate ultraviolet light-induced Fas aggregation in M624 melanoma cells. *Photochem Photobiol* 82:787–792.
18. Perez-Lopez ME, Curiel T, Gomez JG, Jorge M (2007) Role of pegylated liposomal doxorubicin (Caelyx) in the treatment of relapsing ovarian cancer. *Anticancer Drugs* 18:611–617.
19. Rotolo JA, *et al*. (2005) Caspase-dependent and -independent activation of acid sphingomyelinase signaling. *J Biol Chem* 280:26425–26434.
20. Erdreich-Epstein A, *et al*. (2002) Ceramide signaling in fenretinide-induced endothelial cell apoptosis. *J Biol Chem* 277:49531–49537.
21. Cao Y, Pearman AT, Zimmerman GA, McIntyre TM, Prescott SM (2000) Intracellular unesterified arachidonic acid signals apoptosis. *Proc Natl Acad Sci USA* 97:11280–11285.
22. Erdreich-Epstein A, *et al*. (2000) Integrins $\alpha_v\beta_3$ and $\alpha_v\beta_5$ are expressed by endothelium of high-risk neuroblastoma and their inhibition is associated with increased endogenous ceramide. *Cancer Res* 60:712–721.
23. Erdreich-Epstein A, *et al*. (2005) Endothelial apoptosis induced by inhibition of integrins $\alpha_v\beta_3$ and $\alpha_v\beta_5$ involves ceramide metabolic pathways. *Blood* 105:4353–4361.
24. Giovannoni S, Stingl U (2007) The importance of culturing bacterioplankton in the 'omics' age. *Nat Rev Microbiol* 5:820–826.
25. Giovannoni SJ, Stingl U (2005) Molecular diversity and ecology of microbial plankton. *Nature* 437:343–348.
26. Moore RE (1981) Constituents of blue-green algae. *Mar Nat Prod: Chem Biol Perspect* 4:1–52.
27. Burja AM, Banaigs B, Abou-Mansour E, Grant Burgess J, Wright PC (2001) Marine cyanobacteria: A prolific source of natural products. *Tetrahedron* 57:9347–9377.
28. Helfer B, *et al*. (2006) Caspase-8 promotes cell motility and calpain activity under nonapoptotic conditions. *Cancer Res* 66:4273–4278.
29. Schimmer AD, *et al*. (2006) Identification of small molecules that sensitize resistant tumor cells to tumor necrosis factor-family death receptors. *Cancer Res* 66:2367–2375.
30. Kasibhatla S, *et al*. (2005) A role for transferrin receptor in triggering apoptosis when targeted with gambogic acid. *Proc Natl Acad Sci USA* 102:12095–12100.
31. Kondoh M, *et al*. (2004) Kaurene diterpene induces apoptosis in human leukemia cells partly through a caspase-8-dependent pathway. *J Pharmacol Exp Ther* 311:115–122.
32. Santana P, *et al*. (1996) Acid sphingomyelinase-deficient human lymphoblasts and mice are defective in radiation-induced apoptosis. *Cell* 86:189–199.
33. Torchilin VP (2006) Multifunctional nanocarriers. *Adv Drug Deliv Rev* 58:1532–1555.
34. Teitz T, *et al*. (2000) Caspase 8 is deleted or silenced preferentially in childhood neuroblastomas with amplification of MYCN. *Nat Med* 6:529–535.
35. Lawson ND, Weinstein BM (2002) In vivo imaging of embryonic vascular development using transgenic zebrafish. *Dev Biol* 248:307–318.
36. Nusslein-Volhard C, Dahm R, eds (2003) *Zebrafish: A Practical Approach* (Oxford Univ Press, Oxford).
37. Storgard C, Mikolon D, Stupack DG (2005) Angiogenesis assays in the chick CAM. *Methods Mol Biol* 294:123–136.
38. Torres VA, *et al*. (2006) Caveolin-1 controls cell proliferation and cell death by suppressing expression of the inhibitor of apoptosis protein survivin. *J Cell Sci* 119:1812–1823.